**Zeitschrift:** Helvetica Physica Acta
**Band:** 61 (1988)
**Heft:** 4

**Artikel:** Structural, thermal and magnetic properties of the YBa_2Cu_3O_6.9 superconductor prepared by citrate pyrolysis

**Autor:** Junod, A. / Bezinge, A. / Cattani, D.

**DOI:** https://doi.org/10.5169/seals-115950

Helvetica Physica Acta, Vol. 61 (1988) 460–469 0018–0238/88/040460–10$1.50 + 0.20/0


# Structural, thermal and magnetic properties of the $YBa_2Cu_3O_{6.9}$ superconductor prepared by citrate pyrolysis

By A. Junod, A. Bezinge, D. Cattani, M. Decroux, D. Eckert, M. François,[1]) A. Hewat,[2]) J. Muller and K. Yvon[1])

Département de physique de la matière condensée, Université de Genève, CH-1211 Genève 4 (Switzerland)

(5. II. 1988)

*In honor of Martin Peter's 60th birthday.*

*Abstract.* A batch of samples prepared by citrate pyrolysis and submitted to optimized heat treatments is characterized by metallographic investigations, X-ray (300 K) and neutron diffraction (5–320 K), and measurements such as macroscopic density, resistivity, a.c. susceptibility, normal-state d.c. susceptibility, Meissner effect, and high resolution specific heat (1–300 K).

These samples show improved properties compared to those prepared by solid-state techniques, e.g. larger Meissner effect (field cooling), and a well-defined specific heat jump at $T_c$ (57 mJ/(K$^2$ mole)).

High resolution neutron diffraction experiments ($(\sin\Theta/\lambda)_{max} = 0{\cdot}91$ Å$^{-1}$) show that about 9% of the O(4) atoms on the so-called Cu–O chains are missing and that the remaining O(4) atoms are displaced by about 0.10 Å perpendicular to the chain axis.

## Introduction

Within a very short time after the discovery of its outstanding superconducting properties [1, 2], the oxygen-deficient triple layer perovskite $YBa_2Cu_3O_7$ ('YBCO') was extensively characterized by numerous physical measurements. Most studies, including our early report [3] refer to samples prepared by the usual ceramic method, i.e. appropriate oxide, carbonate, nitrate or oxalate powders are mixed, calcined, sintered and oxidized with intermediate grindings. The ultimate sample homogeneity and density that may be obtained by solid-state reactions is limited, however, with a possible detrimental effect on critical current densities. This explains a growing interest in alternative techniques: coprecipitation of nitrates [4], oxalate-, carbonate-, and citrate gel synthesis [5], citrate pyrolysis [6], controlled precipitation of colloids by freeze-drying [7], sol-gel processes [7],

[1]) Laboratoire de cristallographie, Genève.
[2]) Institut Laue-Langevin, Grenoble.

precipitation of acetate solutions [8], etc. Most of the above-mentioned papers emphasize chemical rather than physical aspects; so the present situation is such that a huge amount of physical measurements have been performed on samples prepared by a single technique on one hand, and a wealth of new chemical methods have been put forward with limited physical characterization on the other hand. The purpose of this paper is to fill the gap by presenting a comprehensive structural and physical characterization of an optimized sample obtained by the citrate pyrolysis technique, including microstructural examinations, X-ray diffraction, high-resolution neutron diffraction from 5 K to room temperature, resistivity, a.c. susceptibility, normal-state d.c. susceptibility, Meissner effect, and specific heat from 1 K to room temperature. These measurements will be only briefly commented upon in this paper; the reader will be directed to specialized publications for a detailed analysis of specific measurements. We rather intend to show qualitatively which parameters can be expected to change when improved preparation techniques are used, and which ones are intrinsic.

## Sample preparation

Fifteen identical samples weighing 0.5 gram each (sample codes J444a–J444o) were prepared in a single run. The synthesis essentially follows the steps given by Blank et al. [6]. The starting products, CuO (>99%), $Y_2O_3$ (99.999%) and $BaCO_3$ (>99%), all from Fluka A.G., are weighted and dissolved in equal amounts of hot nitric acid. Water addition helps the dissolution of $BaCO_3$. After thorough mixing, citric acid is added in the proportion of 1 gram to 1 ml $NHO_3$ (85%). The blue solution is then neutralized with ammonia (25%), monitoring the pH with a digital pH-meter calibrated against a buffer solution (pH = 7). The solution is evaporated on a hot plate in an oversized beaker until spontaneous combustion occurs. The resulting dark expanded foam, consisting of sub-micron particles, is lightly pressed, heated *in vacuo* at 400°C to remove organic contaminants and calcined on a Pt foil at 950°C in flowing oxygen during 18 hours. Neither the heating nor the cooling rates are controlled at this stage. The sample is then crushed, pressed into pellets at about 3 kbar, sintered in flowing oxygen at 980°C during 17 h, and cooled at the controlled rate of −50°C/h down to room temperature.

A detailed account of the optimization procedure is given elsewhere [9]. The crucial points are the sub-micron initial particle size, the high sintering temperature that favours densification, and the slow cooling rate that ensures full tetragonal-orthorhombic structural transformation and high oxygen uptake. The final macroscopic density ranges from 5.65 to 5.92 g/cm$^3$ (7–11% porosity).

Microstructural examinations confirm the low porosity (Fig. 1). Typical grain sizes range from 10 to 500 $\mu$m; no impurity phase is visible at the grain boundaries. A careful examination of the crystallites under polarized light reveals complete twinning.

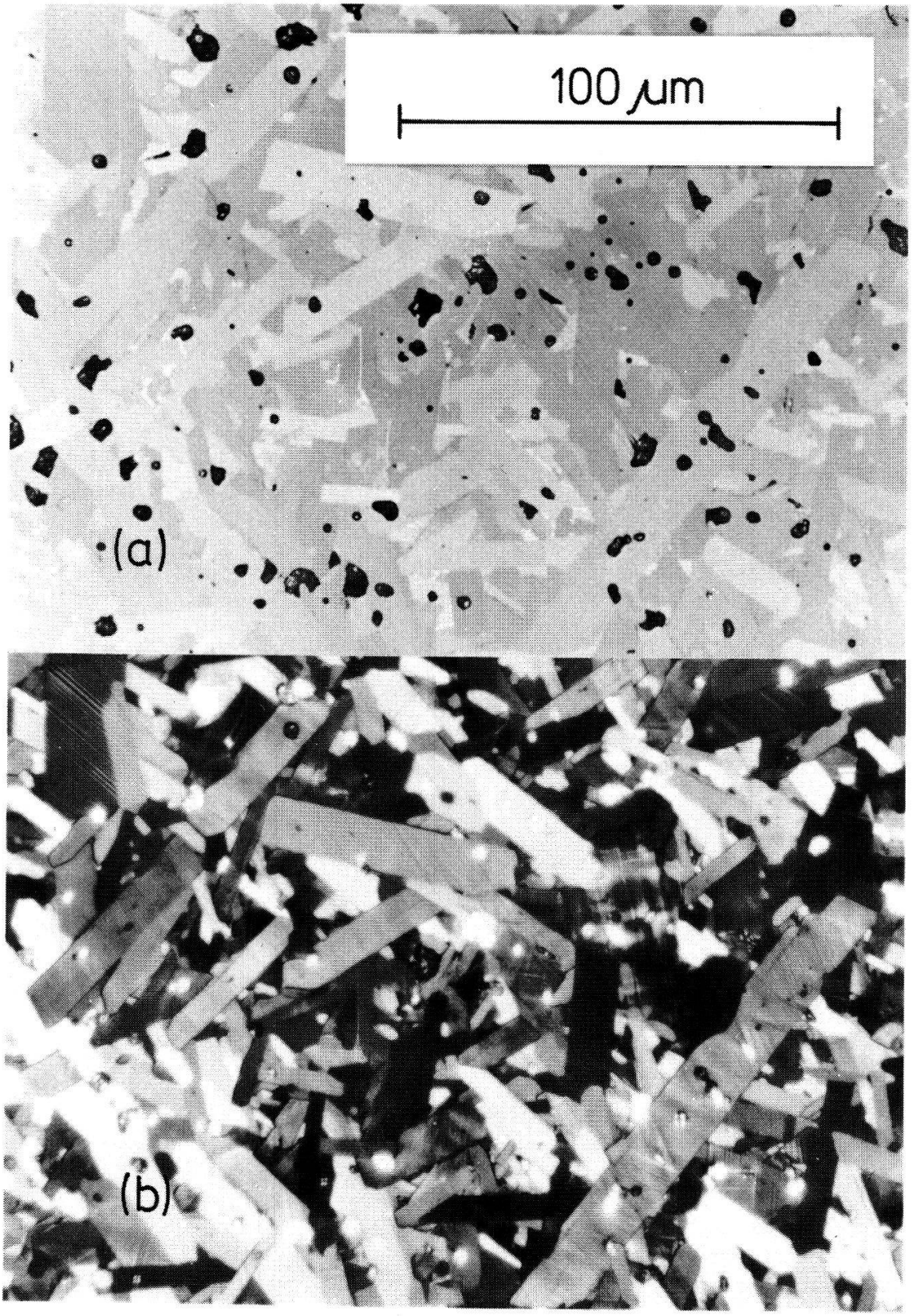


Figure 1
Microstructure of YBCO prepared by citrate pyrolysis. (a), non-polarized; (b) polarized white light. Dark spots in (a), which appear in white in (b), are pores.

## Results and discussion

### 1. *X-ray and neutron diffraction*

The X-ray diffraction experiments are performed by the GUINIER technique (CuK$\alpha$ radiation) at room temperature. The patterns are indexed on the known orthorhombic cell with the following parameters: $a = 3.8179(7)$, $b = 3.8868(9)$, $c = 11.676(2)$ Å. No extra lines indicative of impurity phases are found. A comparison with a previous study [10] shows a 0.2% reduction of the unit cell volume and a slight increase of the orthorhombic distortion, $2(b - a)/(b + a) = 0.0179(4)$ instead of 0.0170. Both are essentially traceable to a contraction of the cell edge along the $a$ axis, which is due to a higher occupancy of the O(4) 'chain' site on the $b$ axis.

The average structure of orthorhombic, superconducting YBCO has been characterized from numerous neutron powder diffraction experiments (for a review see [11]). A structural detail which was not completely clarified is the exact distribution of the oxygen atoms O(4) on the so-called 'linear Cu–O chains' running along the $b$ axis.

The neutron diffraction measurements are performed in the temperature range of 5–320 K on the new high-resolution powder diffractometer D2B at ILL (Grenoble). Details will be reported elsewhere [12]. The structure refinements are performed by the Rietveld method. Except for the oxygen position O(4) (see below) the structure model used is that described previously [10]:

space group Pmmm (No. 47)
Ba in 2$t$ (1/2, 1/2, $z$; $z = 0.185$)
Y in 1$h$ (1/2, 1/2, 1/2)
Cu(1) in 1$a$ (0, 0, 0)
Cu(2) in 2$q$ (0, 0, $z$; $z = 0.355$)
O(1) in 2$q$ (0, 0, $z$; $z = 0.159$)
O(2) in 2$s$ (1/2, 0, $z$; $z = 0.377$)
O(3) in 2$r$ (0, 1/2, $z$; $z = 0.378$)

As to O(4), a split-atom model is used. The O(4) atoms are shifted away from position 1$e$ (0, 1/2, 0, point symmetry mmm) on the Cu–O chain axis and displaced along [100] (i.e. perpendicular to the Cu–O chain axis) to the position 2$k$ ($x$, 1/2, 0; $x = 0.025(2)$; point symmetry 2 mm), assuming statistical occupancy of about 0.5, and isotropic temperature factors.

The refinements converge at a lower residual ($R_F \simeq 3\%$) than those for the earlier sample studied in Ref. [10] ($R_F \simeq 5.3\%$). The results show that about 9% of the O atoms on the Cu–O chains are missing. This value does not significantly change as a function of temperature, and there is no evidence for the presence of other O atoms in the structure. Thus the compound has the stoichiometry $YBa_2Cu_3O_{6.91}$. The displacement parameter, $x$, of the split-atom position O(4) refines consistently to non-zero values. Thus the O(4) atoms are definitely not situated on the Cu–O chain axis as was assumed previously but are displaced by

about 0.10(1) Å away from the chain axis. The reason why these displacements have not been seen in earlier structure refinements is presumably due to a lack of resolution of the diffraction data. Furthermore, anomalies are observed for these displacements and also for some other structural parameters around 90 K and 240 K, which are described elsewhere [12].

## 2. *Resistivity*

The resistance is measured with the 4-leads a.c. technique, using a current density of about 50 mA/cm$^2$. Contact resistances below 0.1 Ω are obtained attaching the leads with silver-filled epoxy (EpoTek HE20) baked at 300–400°C during half an hour.

The high temperature behaviour is metallic, as generally found in well oxidized samples; the ratio between the resistance at 300 K and 100 K is 2.65 and the room temperature resistivity is $600 \pm 50\ \mu\Omega$cm. The midpoint of the superconducting transition is 95.1 K, as shown in Fig. 2, and the resistance drops to zero within experimental resolution at 94.3 K. With a width of 0.58 K (10%–90%), the resistive transition is sharper than for any other known polycrystalline YBCO material. This value of $T_c$ is somewhat higher than those observed with other experiments. However, an ageing effect was observed: $T_c$ dropped to 92 K within one month after the measurements reported here were performed, a value in good agreement with the onset of the specific heat anomaly (Fig. 2).

## 3. *A.c. susceptibility*

The a.c. susceptibility is measured in a low external field of 0.01 Oe r.m.s. at 73 Hz, sweeping up the temperature from 5 to 100 K at a rate of 15 K/h. Figure 2

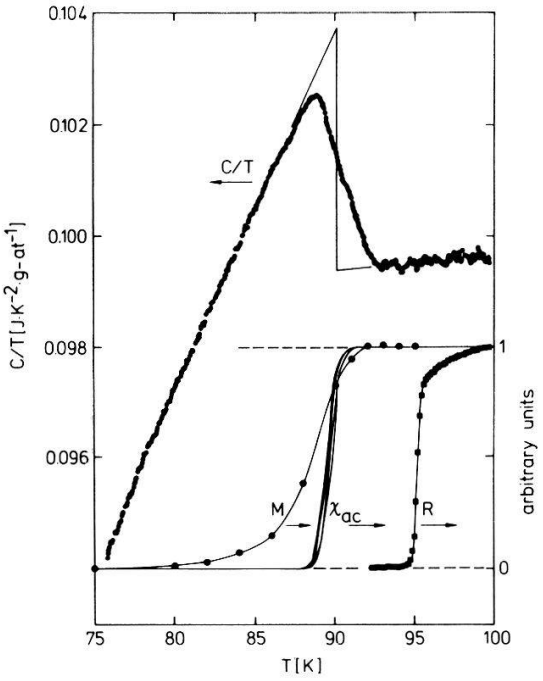


Figure 2
Upper curve: specific heat divided by the temperature $C/T$ as a function of the temperature, measured data and idealized specific heat jump at $T_c$ (1 g-at = 1/13 mole). Lower curves: Meissner magnetization $M$ (cooling curve in a constant field $H = 17$ Oe), a.c. susceptibility $\chi_{ac}$ at $H_{rms} = 0.01$ Oe for five samples of the same batch, and resistance $R$ as a function of temperature close to $T_c$. The ordinates of the last three curves are normalized at $T = 100$ K and $T = 5$ K.

displays the diamagnetic shielding transition for five samples selected at random from the batch (J444A–E). The transition midpoint, 89.5 K on the average, and the transition width, typically 1.5 K, are not optimal and we have observed 91.3 K and 0.39 K (10%–90%), respectively, in another batch (J442) obtained by the same preparation technique.

Although no better results for *chemically* prepared samples have been published so far, similarly sharp transitions have been obtained for samples prepared by solid-state reactions [13]. Such a shielding measurement does not make the difference between partially and fully superconducting samples and further characterization is necessary.

## 4. *Meissner effect*

The Meissner effect is measured in a SQUID magnetometer by cooling the sample from above its transition temperature in a constant magnetic field of 17 Oe. The diamagnetic signal (Fig. 2) corresponds to 60% of the complete flux expulsion ($-1/4\pi$) below 80 K, after correction for the demagnetizing factor (raw values: 70% and 83%, depending on the field direction). This is the largest Meissner fraction we have observed so far for YBCO samples in such a field. The specification of the field is of importance; Krusin-Elbaum et al. [14] have reported a dramatic decrease by a factor >2.5 of the Meissner fraction between 50 mOe and ~15 Oe in their single crystal.

## 5. *Normal-state susceptibility*

The normal-state susceptibility is measured between 100 and 250 K in a magnetic field of 20 kOe using the same apparatus (Fig. 3). It is field

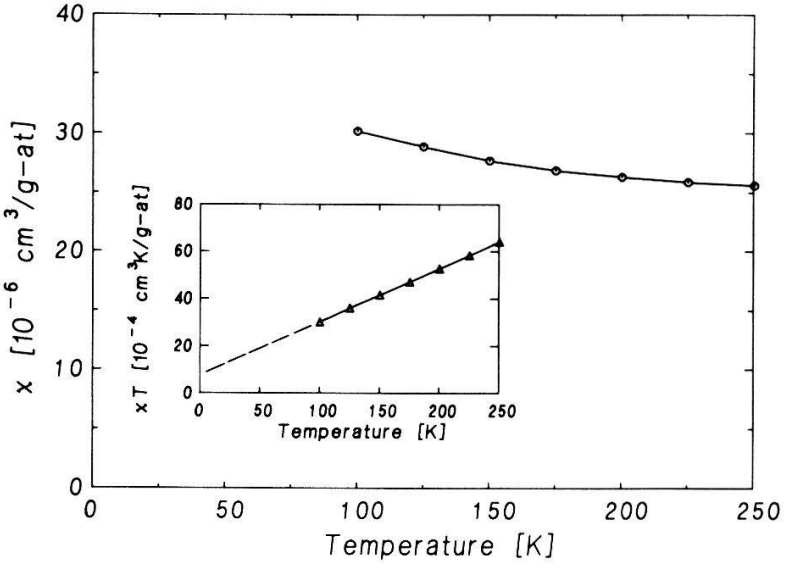


Figure 3
Normal state susceptibiltiy per g-at above $T_c$ in a magnetic field of 20 kOe. The inset shows $\chi T$ as a function of $T$: the extrapolated ordinate gives the Curie term and the slope gives the constant term $\chi_0$.

independent, in view of the negligible amount of ferromagnetic impurities detected in previous samples. The slope of $\chi \cdot T$ as a function of $T$ (inset of Fig. 3) gives the temperature independent component of the susceptibility $\chi_0 = 22.5 \cdot 10^{-6}\,\mathrm{cm^3/g\text{-}at}$, which is the largest value that we have observed so far. Assuming localized $Cu^{++}$ magnetic moments, the Curie contribution corresponds to 0.8% $Cu^{++}/Cu^{total}$. This is close to the minimum value of paramagnetic impurities we have detected until now, 0.4% in a sample also prepared by citrate pyrolysis (J442d).

## 6. *Low temperature specific heat*

The low temperature specific heat is measured from 1.4 K to 10 K by a thermal relaxation method on a 94 mg sample. The addenda contribution is measured separately and subtracted: it represents 4% to the total heat capacity at 1.4 K, 28% at 10 K.

In Fig. 4 we present the specific heat in a $C/T$ vs. $T^2$ plot. Assuming that in the range $T^2 = 40$ to $100\,\mathrm{K^2}$ the specific heat is the sum of a linear term and a cubic lattice term, then a straight-line extrapolation to $T = 0$ yields a linear coefficient $\gamma = 5.6\,\mathrm{mJ/(K^2\,mole)}$ and a Debye temperature $\Theta_D = 410\,\mathrm{K}$.

The non-zero $\gamma$ value and the upturn in $C/T$ are surprizing, as one expects the specific heat of a superconductor at $T \ll T_c$ to be the sum of an exponential electronic term and a cubic lattice term. This anomalous behaviour has been reported in all the published YBCO low temperature specific heat results (for a complete list of references see ref. [15]); extensive studies that we have done on the possible impurity phases lead us to believe that these anomalies are largely due to the presence of small amounts of $BaCuO_2$ in the measured samples [15]. This means that the lower the specific heat $C/T$ in the 1–10 K range (i.e. the lower the value of $\gamma$ and the higher the value of $\Theta_D$), the higher the purity of the sample. The published values of the linear coefficient vary between 4 and 11 $\mathrm{mJ/(K^2\,mole)}$, with an average of about 8.3 $\mathrm{mJ/(K^2\,mole)}$; $\Theta_D$ values from 352 to 430 K have been observed with an average of 380. With $\gamma = 5.6\,\mathrm{mJ/(K^2\,mole)}$ and $\Theta_D = 410\,\mathrm{K}$, the samples prepared by citrate pryolysis certainly contain only small amounts of $BaCuO_2$, CuO, etc.

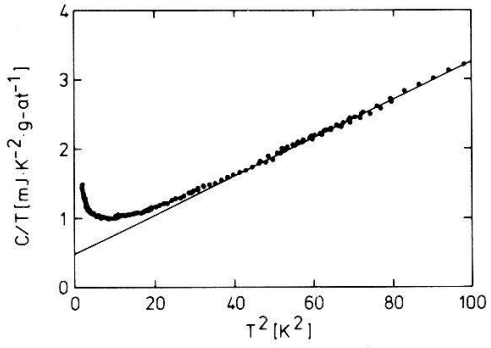


Figure 4
Specific heat divided by the temperature vs. temperature squared from 1.2 to 10 K.

## 7. *Specific heat jump*

The heat capacity above 30 K is measured by a continuous heating adiabatic method, essentially a computerized version of an early analog design [16]. With a heating rate of 1.4 mK/s near $T_c$, the data density reaches 35 points/K and the scatter, which is typically 0.05% below $T_c$, suddenly jumps to 0.25% (peak-to-peak) just above $T_c$ for some unexplained reason. Structural instability or strain releases are suspected.

The specific heat jump at $T_c$ is better defined than for any sample prepared by solid-state reaction (Fig. 2). The difference between the maximum value of $C/T$ just below $T_c$ and $C/T$ at 95 K, without idealization, is an objective measure of the sample homogeneity. In the present case, the difference is 40 mJ/(K$^2$ mole), to be compared with 7 [17] (we have re-plotted their results in the form $C/T$ vs. $T$ and taken the max/min values), 19 [3], 23 [18], 24 [19], 25 [20], 27 [21] (40 if the continued decrease *above* $T_c$ from 95 and 100 K is taken into account), 29 [22], 32 [23], and 32 [24]. The extrapolation to obtain the *idealized* $\Delta C/T_c$ from smeared transitions is largely a matter of taste; the simple linear (entropy conserving) extrapolations of Fig. 2 yield $\Delta C/T_c =$ 57 mJ/(K$^2$ mol).

Since the anomaly of the specific heat at $T_c$ is the only bulk measurement of the superconducting volume, one can conclude that the optimized citrate pyrolysis method is suited to obtain homogeneous samples.

## 8. *High temperature specific heat*

The specific heat in the range 30–300 K is shown in Fig. 5. Besides freezing of the silicon grease used to attach the sample, at 236 K, no anomaly is seen between $T_c$ and room temperature. The failure to reach the equipartition value (24.94 J/(K · g-at)) at room temperature in spite of the presence of electronic and anharmonic contributions expresses the fact that the phonon spectrum extends to very high energies, of the order of 80 meV. The room-temperature specific heat is somewhat smaller than for less oxidized samples [19], indicating stiffer bonds probably due to a reduced number of vacancies on the O(4) sites.

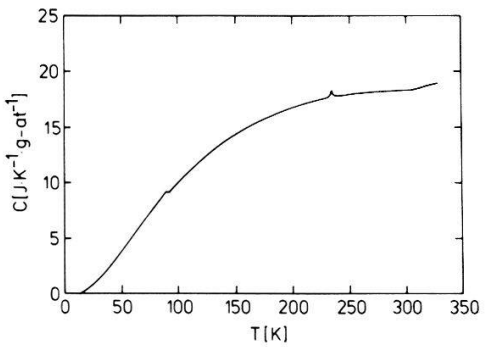


Figure 5
Specific heat vs. temperature up to room temperature. The solid line is drawn after ~5000 data points with typical 0.1% scatter.

## Conclusion

The samples prepared by citrate pyrolysis, using higher than usual reaction temperatures and a slow cooldown under oxygen atmosphere, are characterized by (1) a low porosity, (2) a large grain size, (3) a high purity according to microstructural examinations, X-ray patterns, neutron diffraction, normal-state susceptibility and low-temperature specific heat, (4) a high and sharp superconducting transition temperature (as measured by resistivity, a.c. susceptibility, Meissner flux expulsion and specified heat), (5) a large Meissner fraction, (6) a high and almost temperature-independent normal-state susceptibility, (7) a large specific heat jump at $T_c$, and (8) a smooth specific heat up to room temperature. All these characteristics reveal a real progress as compared to earlier samples prepared by solid-state reactions. Until now, this synthesis technique does not succeed however in obtaining critical current densities above a few hundred A/cm$^2$ at 4 K, and does not affect $T_c$.

REFERENCES

[1] M. K. Wu, J. R. Ashburn, C. J. Torng, P. H. Hor, R. L. Meng, L. Gao, Z. J. Huang, Y. Q. Wang and W. C. Chu, Phys. Rev. Lett *8*, 908 (1987).
[2] Z. Zhao, L. Chen, Q. Yang, Y. Huang, G. Chen, R. Tang, G. Liu, C. Cui, L. Chen, L. Wang, S. Guo, S. Li and J. Bi, Kexue Tongbao *6* (1987).
[3] A. Junod, A. Bezinge, T. Graf, J.-L. Jorda, J. Muller, L. Antognazza, D. Cattani, J. Cors, M. Decroux, Ø. Fischer, M. Banovski, P. Genoud, L. Hoffmann, A. A. Manuel, M. Peter, E. Walker, M. François and K. Yvon, Europhys. Lett. *4*, 247 (1987).
[4] K. Koyama, T. Tsunemi, T. Miki, A. Oota, A. Ueno and S. Noguchi, Jap. J. of Appl. Phys. *26* suppl. 26-3, 1075 (1987), and additional information on their poster CN24, XVIIIth Int. Conf. on Low Temp. Phys., Kyoto 1987.
[5] M. Hirabayashi, H. Ihara, N. Terada, K. Senzaki and Y. Kimura, poster CN17, XVIIIth Int. Conf. on Low Temp. Phys., Kyoto 1987 (unpublished).
[6] D. H. A. Blank, H. Kruidhof and J. Flokstra, J. of Physics D: Applied Physics *21*, 226 (1988).
[7] P. Barboux, J. M. Tarascon, L. H. Greene, G. W. Hull and B. G. Bagley, to appear in J. Appl. Phys.
[8] P. J. Melling, S. L. Swartz, M. Pardavi-Horvath and E. W. Collings, to be published in *Advances in Cryogenic Engineering (Materials), Vol.* 34.
[9] A. Junod, A. Bezinge and J. Muller, to be published.
[10] M. François, E. Walker, J.-L. Jorda, K. Yvon and P. Fischer, Sol. State Commun. *63*, 1149 (1987).
[11] K. Yvon, Z. Physik (1988), to be published.
[12] M. François, A. Junod, K. Yvon, P. Fischer, J. J. Capponi, P. Strobel, M. Marezio and A. W. Hewat, to be published.
[13] A. Junod, A. Bezinge, D. Cattani, J. Cors, M. Decroux, Ø. Fischer, P. Genoud, L. Hoffmann, J.-L. Jorda, J. Muller and E. Walker, Jap. J. of Appl. Phys. *26* suppl. 26-3, 1021 (1987).
[14] L. Krusin-Elbaum, A. P. Malozemoff and Y. Yeshurun, preprint.
[15] D. Eckert, A. Junod, A. Bezinge, T. Graf and J. Muller, to be published.
[16] A. Junod, J. Phys. E: Sci. Instrum. *12*, 945 (1979).
[17] S. E. Inderhees, M. B. Salamon, T. A. Friedmann and D. M. Ginsberg, preprint.
[18] J. C. van Miltenburg, A. Schuijff, K. Kadowaki, M. van Sprang, J. Q. A. Koster, Y. K. Huang, A. A. Menovsky, and H. Barten, to appear in Physica.
[19] A. Junod, A. Bezinge, D. Cattani, J. Cors, M. Decroux, Ø. Fischer, P. Genoud, L. Hoffmann, J.-L. Jorda, J. Muller and E. Walker, Jap. J. of Appl. Phys. *26* suppl. 26-3, 1119 (1987).

[20] M. V. NEVITT, G. W. CRABTREE and T. E. KLIPPERT, to appear in Phys. Rev. Rapid Comm.
[21] C. AYACHE, B. BARBARA, E. BONJOUR, R. CALEMCZUK, M. COUACH, J. H. HENRY and J. ROSSAT-MIGNOD, to appear in Solid State Commun.
[22] N. E. PHILLIPS, R. A. FISHER, S. E. LACY, C. MARCENAT, J. A. OLSEN, W. K. HAM, A. M. STACY, J. E. GORDON and M. L. TAN, Proceedings of the Yamada Conference on Superconductivity in highly correlated fermion systems, Sendai 1987 (preprint).
[23] O. BECKMAN, L. LUNDGREN, P. NORDBLAD, L. SANDLUND, P. SVEDLINH, T. LUNDSTRÖM and S. RUNDQVIST, to appear in Phys. Lett.
[24] M. ISHIKAWA, T. TAKABATAKE and Y. NAKAZAWA, Proceedings of the Yamada Conference on Superconductivity in highly correlated fermion systems, Sendai 1987 (preprint).